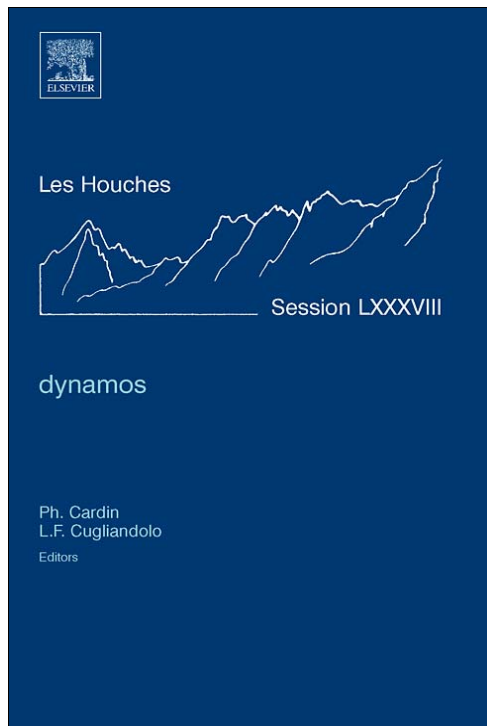


**Provided for non-commercial research and educational use only.  
Not for reproduction, distribution or commercial use.**

This chapter was originally published in the book *Les Houches, Session LXXXVIII, 2007, Dynamos*. The copy attached is provided by Elsevier for the author's benefit and for the benefit of the author's institution, for noncommercial research, and educational use. This includes without limitation use in instruction at your institution, distribution to specific colleagues, and providing a copy to your institution's administrator.



All other uses, reproduction and distribution, including without limitation commercial reprints, selling or licensing copies or access, or posting on open internet sites, your personal or institution's website or repository, are prohibited. For exceptions, permission may be sought for such use through Elsevier's permissions site at:

<http://www.elsevier.com/locate/permissionusematerial>

From Yannick Ponty, Numerical modeling of liquid metal dynamo experiments. In: Ph. Cardin, L.F. Cugliandolo, editors, *Les Houches, Session LXXXVIII, 2007, Dynamos*. Amsterdam: Elsevier, 2008, p. 359

ISBN: 978-0-0805-4812-8

© Copyright 2008 Elsevier B.V.

Elsevier

Course 6

**NUMERICAL MODELING OF LIQUID METAL DYNAMO  
EXPERIMENTS**

Yannick Ponty

*Laboratoire Cassiopée UMR 6202, Observatoire de la Côte d'Azur,  
BP 4229, Nice Cedex 04, France*

*Ph. Cardin and L.F. Cugliandolo, eds.  
Les Houches, Session LXXXVIII, 2007  
Dynamos  
© 2008 Published by Elsevier B.V.*

Author's personal copy

## Contents

1. Preamble	363
2. Introduction	363
3. Numerical method	364
3.1. The periodic box numerical experiment	364
3.2. Fundamentals equations	364
3.3. Non dimensional numbers	365
3.4. Numerical schemes	366
3.5. Turbulence and subgrid modeling	366
4. Magnetic induction	367
5. Linear dynamo onset	369
5.1. Static or turbulent kinematic dynamo	369
5.2. Taylor–Green dynamo	370
6. Non linear behavior	373
6.1. Subcritical dynamo	373
6.2. On-Off intermittency dynamo	375
7. Perspective	377
8. Acknowledgements	378
References	378

Author's personal copy

## 1. Preamble

Dynamo action, the self amplification of magnetic field due to the stretching of magnetic field lines by a fluctuating flow, is considered to be the main mechanism for the generation of magnetic fields in the universe [1]. In this respect many experimental groups have successfully reproduced dynamos in liquid sodium laboratory experiments [2–8]. The induction experiments [9–18] studying the response of an applied magnetic field inside a turbulent metal liquid also represent a challenging science. With or without dynamo instability the flow of a conducting fluid forms complex system, with a large degrees of freedom and a wide branches of non linear behaviors.

## 2. Introduction

For laboratory experiments, the numerical prediction of the dynamo threshold in realistic conditions is still out of reach. Nonetheless, the experiments [2] in Riga and Karlsruhe [5] found the onset to be remarkably close to the values predicted from numerical simulations based on the mean flow structure [19, 20], and this despite the fact that the corresponding flows are quite turbulent.

This has led several experimental groups seeking dynamo action in less constrained geometry, eventually leading to richer dynamical regimes [7, 8], to optimize the flow forcing using kinematic simulations based on mean flow measurements [21, 22]—the advantage being that mean flow profiles can be measured in the laboratory.

Actually, there are efforts in numerical methods to take account of real geometries and the shapes of the experimental apparatus, the effect of the fluid and the magnetic boundary conditions, the use of finite element, finite volume and finite difference mesh schemes [23–28]. However as we will shown in this lecture, it is possible to numerically study some aspects of experimental dynamo behavior without boundary conditions in a three-dimensional periodic space, and we shall seek the respective role of mean flow and the turbulence in this.

### 3. Numerical method

#### 3.1. The periodic box numerical experiment

Incompressible turbulent flows have been studied intensively in a periodic space, which is a classical mathematical framework for analysis and theory [29, 30]. The energy cascade, the organisation of the energy transfer between the different scales are naturally handle in spectral space. The Navier–Stoke equation accumulates the maximum number of symmetries in a periodic space and this lack of real boundaries has been used for numerical simulations of isotropic and homogeneous turbulence [31]. The pseudo-spectral numerical method [33–36] is a global method and probably the most precise numerical method for a fix mesh size. For all these reasons, in this lecture we will concentrate on numerical simulations of incompressible conductor flow in a fully three-dimensional periodic box.

#### 3.2. Fundamentals equations

Let us work with the incompressible magnetohydrodynamic equations (3.1)–(3.2)

$$\frac{\partial \mathbf{v}}{\partial t} + \mathbf{v} \cdot \nabla \mathbf{v} = -\nabla \mathcal{P} + \mathbf{j} \times \mathbf{B} + \nu \nabla^2 \mathbf{v} + \mathbf{F}, \quad (3.1)$$

$$\frac{\partial \mathbf{B}}{\partial t} + \mathbf{v} \cdot \nabla \mathbf{B} = \mathbf{B} \cdot \nabla \mathbf{v} + \eta \nabla^2 \mathbf{B}, \quad (3.2)$$

together with  $\nabla \cdot \mathbf{v} = \nabla \cdot \mathbf{B} = 0$ ; a constant mass density  $\rho = 1$  is assumed. Here,  $\mathbf{v}$  stands for the velocity field,  $\mathbf{B}$  the magnetic field (in units of Alfvén velocity),  $\mathbf{j} = (\nabla \times \mathbf{B})/\mu_0$  the current density,  $\nu$  the kinematic viscosity,  $\eta$  the magnetic diffusivity and  $\mathcal{P}$  is the pressure. The forcing term  $\mathbf{F}$  will be chosen between two different forcing,s respectively they are Taylor–Green vortex (TG) [37],

$$\mathbf{F}_{\text{TG}}(k_0) = \begin{bmatrix} \sin(k_0 x) \cos(k_0 y) \cos(k_0 z) \\ -\cos(k_0 x) \sin(k_0 y) \cos(k_0 z) \\ 0 \end{bmatrix}, \quad (3.3)$$

and the ABC flow [38, 39]

$$\mathbf{F}_{\text{ABC}}(k_0) = \begin{bmatrix} A \sin(k_0 z) + C \cos(k_0 y) \\ B \sin(k_0 x) + A \cos(k_0 z) \\ C \sin(k_0 y) + B \cos(k_0 x) \end{bmatrix}, \quad (3.4)$$

with  $A = B = C = k_o = 1$ .

There are several ways to implement a forcing term in the Navier–Stoke equation, but there are two superior, less artificial ways, which correspond to two possible experimental forcings. The first one is used in this lecture, it is called constant forcing or constant torque, where the forcing term in the Navier–Stoke equation is simply add at each time step to the rest of the momentum equation. The other one is the constant velocity, it is implemented generally in the spectral space, imposing constant values for selected wave vectors at each time step.

### 3.3. Non dimensional numbers

We solve the dimensional form of the MHD (3.1)–(3.2) equations, and compute the non dimensional numbers *a posteriori*, using the numerical output quantities. Working with the velocity in  $\text{m s}^{-1}$ , a  $2\pi$  meter box and the viscosity in  $\text{m}^2 \text{s}^{-1}$ , can try to simulate a real experiment however even if we can numerically reach the velocity values close to the experiment values (order one), Unfortunately, we are far away to handle the real viscosity values of water or liquid sodium ( $10^{-6} \text{ m}^2 \text{ s}^{-1}$ ). Actually, we can reach numerical values of the viscosity of  $10^{-2}$  to  $10^{-3} \text{ m}^2 \text{ s}^{-1}$  which is just better than molasses ( $1 \text{ m}^2 \text{ s}^{-1}$ ) or the honey ( $10^{-1} \text{ m}^2 \text{ s}^{-1}$ ).

Nevertheless, we can still define classical non dimensional numbers such as the Reynolds number  $R_v = \frac{L V}{\nu}$  and  $R_m = \frac{L V}{\eta}$  with a characteristic velocity  $V$ , length scale  $L$  and the viscosity  $\nu$  or the magnetic diffusivity  $\eta$ . We choose to use the root mean square velocity  $V_{rms} = \sqrt{2E_v}$  based on the total kinetic energy  $E_v$ , or its average in time for fluctuated flow. We also choose the two following characteristic lengths scale: the integral length scale define by  $L_{int} = \frac{1}{E_v} \sum \frac{E_v(k)}{k} dk$  which measures the largest eddy scale size, where  $E_v(k)$  represent the uni-dimensional isotropic energy density, and the Taylor microscale, the scale where the viscous dissipation begins to affect the eddies,  $L_\lambda = \sqrt{5E_v/\Omega_v}$  with  $\Omega_v = \frac{1}{2} \int (\nabla \times \mathbf{v}(\mathbf{x}, t))^2 dx^3$  is the enstrophy. In the fully turbulence regime, experimental results find the relation  $R_\lambda \sim \sqrt{R_v}$ .

Note two important non dimensional numbers for liquid metal dynamo process: Firstly, the magnetic Reynolds number  $R_m = \frac{L V}{\eta}$  which represents the ratio of the eddy turn over time  $\tau_{NL} = \frac{L_{int}}{V_{rms}}$  and the magnetic diffusion time  $\tau_\eta = \frac{L_{int}^2}{\eta}$ . This number is generally between 10 and 200 which implies that long hydrodynamic simulations are needed to achieved one or two magnetic diffusion times. Secondly, the magnetic Prandtl number  $P_m = \frac{\nu}{\eta}$  which is the ratio of the magnetic diffusion time over the viscous time scale  $\tau_\nu = \frac{L_{int}^2}{\nu}$ . This number is very small ( $10^{-5}$ – $10^{-6}$ ) in liquid metal and this implies high Reynolds number regimes need to be reached to produce a reasonable magnetic Reynolds number above the dynamo onset threshold.

### 3.4. Numerical schemes

In the periodic box, we use the pseudo-spectral method initiated by the work of Orszag (1969, 1972) [32, 35] and Orszag and Patterson (1971) [36]. The success of this method is essential due to the high accuracy and the efficiency of the Fast Fourier Transform (FFT). The linear terms are treated in spectral space, the non linear terms in real space, and the FFT moves the fields between the two mathematical spaces. For the incompressible Navier–Stoke equation, the pressure is eliminated by applying the divergence free operator in Fourier space. This trick greatly simplifies the simulation of incompressible flow, but constrains us to recovering only periodic solutions. We use a “semi-exact” temporal scheme proposed by Basdevant (1982) [40] to implicitly treat the viscous or diffusion terms. This method has been used with success in homogeneous turbulence studies [31]. The equation diffusion system is written in spectral space as

$$\frac{dU_{\vec{k}}}{dt} = -vk^2 U_{\vec{k}} + G_{\vec{k}}(U) \quad (3.5)$$

where  $U_{\vec{k}}$  is the velocity function in the spectral space for the wave vector  $\vec{k}$ . And the solution can be explicitly written with the exponential form as

$$\frac{d e^{vk^2 t} U_{\vec{k}}}{dt} = e^{vk^2 t} G_{\vec{k}}(U_{\vec{k}}(t), t) \quad (3.6)$$

Using the second order of Adams-Basford scheme, the temporal scheme can be written as

$$U_{\vec{k}}(t + \Delta t) = U_{\vec{k}}(t)e^{-vk^2 \Delta t} + e^{-vk^2 \Delta t} \Delta t \left[ \frac{3}{2} G_{\vec{k}}(t) - \frac{1}{2} G_{\vec{k}}(t - \Delta t)e^{-vk^2 \Delta t} \right] \quad (3.7)$$

where  $\Delta t$  is time stepping. If we include the dealiasing there by removing high wave numbers using the 3/2 rule, we get a stable numerical scheme. These methods are described in detail in the chapter 7.2 of the Peyret’s monography [34].

### 3.5. Turbulence and subgrid modeling

Nowadays the largest numerical simulation for the incompressible Navier–Stoke equation in periodic geometry reach  $4096^3$  grid points [41], with a such mesh the kinetic Reynolds number is bounded below  $R_v \sim 65000$  or  $R_\lambda \sim 1200$ . This is still far from the minimum of  $R_v \sim 10^6$  necessary to produce a dynamo in the low magnetic Prandtl number limit. One way around this difficulty is to resort to use Large Eddy Simulations (or LES) [42–45]. Such techniques are widely used in

engineering contexts, as well as in atmospheric sciences and in some case in geophysics and astrophysics. Such subgrid model controls the energy transfer and obtains a larger inertial range, where the energy cascade has a constant dissipation rate. We have used one particular LES model [30,46,47] where the viscosity depends of the modulus of the wave-vectors  $\vec{k}$ . The turbulent viscosity becomes  $\nu(k, t) = \nu_0 H(k) \sqrt{\frac{E(K_{\max}, t)}{K_{\max}}}$  where  $H(k)$  is called a ‘‘cups’’ function equal to unity at large scale and increases the dissipation a high wave number and  $\nu_0$  depends on the forcing and the Kolmogorov constant. This eddy viscosity form is an asymptotic solution of a Navier–Stoke closure approximation. It is possible to take in to account all the closure terms, and solve the full integro-numerical system to obtain a dynamical and more precise LES model [48].

#### 4. Magnetic induction

We consider the induction of a magnetic field in the flows of an electrically conducting fluid at low magnetic Prandtl number and large kinetic Reynolds number. The coupled magnetic and fluid equations (3.1)–(3.2) are solved using a mixed scheme, where the magnetic field fluctuations are fully resolved and the velocity fluctuations at small scale are modeled using a Large Eddy Simulation (LES) scheme as describe in (3.5). We study the response of a forced Taylor–Green flow (eq. (3.3)) to an externally applied field  $B_0$  [49]. In a periodic box, the external magnetic field is implemented in spectral space by feeding energy to the  $k_x = k_y = k_z = 0$  wave vector for the chosen magnetic field component.

Figure 1 shows the kinetic and magnetic spectra, at a given time of the simulation. The kinetic energy spectrum exhibits a  $k^{-5/3}$  Kolmogorov scaling main-

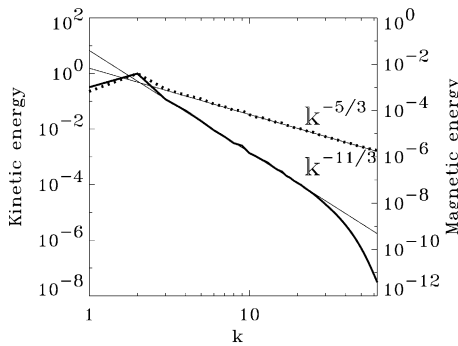


Fig. 1. Magnetic (solid line) and kinetic (dash line) energy spectra.

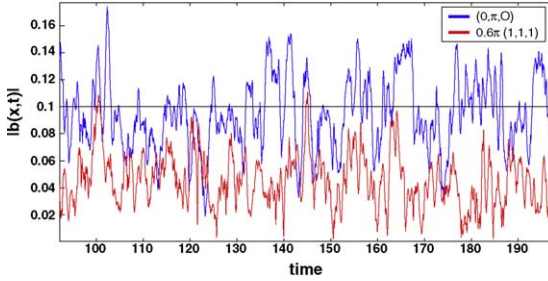


Fig. 2. Time traces of  $|\mathbf{b}(\mathbf{x}, t)|$ , for  $\mathbf{B}_0 = 0.1 \hat{\mathbf{x}}$ , at two fixed points.

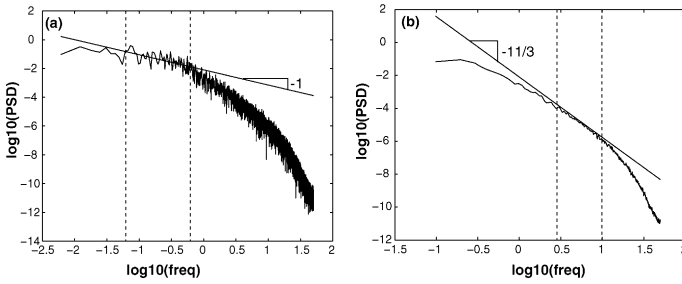


Fig. 3. Power spectral density of the magnetic field fluctuations of  $b_x(\mathbf{x}, t)$  in time, recorded at space location. (a) PSD computed as averages over Fourier transforms calculated over long time intervals ( $164t_0$ ) to emphasize the low frequency behavior; (b) PSD estimated from Fourier transforms over shorter time intervals ( $10t_0$ ). The behavior is identical for the  $b_y(\mathbf{x}, t)$  and  $b_x(\mathbf{x}, t)$  field components.

tained by the LES scheme. The peak at low wave number, also visible on the magnetic field spectrum, is due the large scale TG forcing. The magnetic inertial range is well fitted by a  $k^{-11/3}$  power law in agreement with the Kolmogorov phenomenology [1, 9], where the advection of the external magnetic field is balance by the magnetic diffusion  $\mathbf{B}_0 \nabla \cdot \mathbf{v} \sim \eta \Delta \mathbf{b}$ . Using this numerical “mixed scheme”, we obtain low magnetic Prandtl numbers of  $P_m \sim 10^{-3} - 10^{-4}$ , but the magnetic Reynolds number remains order one.

During the simulation, we record also the velocity and the magnetic fluctuation at fixed points, so as to be able to compare these experimental dates. In Fig. 2, we present a sample of the magnetic fluctuations. The amplitude of the magnetic fluctuations are easily above level of the external magnetic field. As shown in several experiment [9, 13, 17], the liquid metal turbulent flow represent a efficient magnetic amplifier.

In Fig. 3 we plot the power spectra of temporal fluctuations of the magnetic field component  $b_x(\mathbf{x}, t)$  recorded one point fixed. The higher end of the time

spectrum follows a  $f^{-11/3}$  behavior ( $f$  is signal time frequency), as can be expected from the spatial spectrum using the Taylor hypothesis of “frozen” field lines advected by the mean flow [9]. For frequencies between roughly  $1/t_0$  and  $1/10t_0$ , where the dynamical time  $t_0$  is set to the magnetic diffusion time scale. The time spectrum develops a  $1/f$  behavior (Fig. 3b), which is observed in experiment [13]. Note that the  $k^{-1}$  power law is not present on the spatial spectrum in Fig. 1.

## 5. Linear dynamo onset

### 5.1. Static or turbulent kinematic dynamo

The dynamo effect is an instability, initiated by a magnetic seed, where the geometric properties and the dynamics of the fluid amplify the magnetic field energy exponentially. We call this regime the linear phase, or kinematic dynamo. We must distinguish between the mathematical/static kinematic dynamo with the turbulent/dynamical kinematic dynamo. In the first case, a velocity defined mathematically or an time averaged velocity field from a fluid experiment or a numerical simulations are constant in time and inserted in the induction equation. In the second case the velocity field evolves in time its evolution coming from a numerical solution of the Navier–Stokes equation. However in the both cases the Lorentz force is not present, and so there is no back reaction on the flow.

There are historical examples of mathematical kinematic dynamos with the ABC flow, this being a helical Beltrami flow with chaotic Lagrangian trajectories [39]. The kinematic dynamo instability of the ABC flow, even with one of the amplitude coefficients set to zero ( $2^{1/2}$  dimensional flow) [50, 51] has been studied intensively [52–56], especially for fast dynamo investigation [57–61]. The magnetic field grows near the stagnation point of the flow, producing “cigar” shape structures aligned along the unstable manifold. For the ABC with all the coefficients equal to the unity ( $A = B = C = k_0 = 1$ ), there are two windows of dynamo instability [52, 53], which disappear when the velocity field occurs on smaller scales ( $k_0 > 2$ ) [54].

In the dynamic regime, where the velocity is fully resolved numerically at constant forcing  $F_{ABC}$  (3.4), and above a critical Reynolds number, the hydrodynamic system becomes unstable. After the first bifurcation, further increase of the kinematic Reynolds number, leads the system to jump to different attractors [62–65], until finally the fully turbulent regime is reached. Then the dynamo onset increases rapidly with the Reynolds number, until finally reaching a plateau [66].

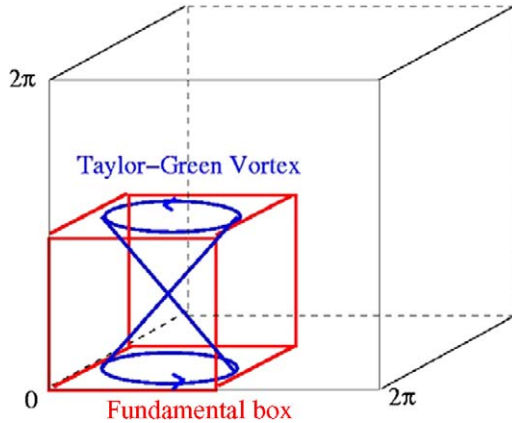


Fig. 4. Representation of fundamental Taylor–Green box in a fully periodic box.

### 5.2. Taylor–Green dynamo

The Taylor–Green flow included height fundamental box (for  $k_0 = 1$ ) (see Fig. 4). In the fundamental box, the Taylor–Green vortex has similar hydrodynamic properties to the experimental Von Kàrmàn vortex [67]. It has been demonstrated that this forcing can produce a numerical dynamo [68, 69] at low Reynolds number and with a magnetic Prandtl number order one. Note the mathematical flow itself can not be a kinematic dynamo, it has one velocity component set to zero (eq. 3.3). The system needs the recirculation created by the inertial term, producing a three-dimensional velocity necessary for the dynamo instability. When the Reynolds number increases, the onset of the dynamo also increases until is reaching a plateau [70] (see Fig. 5).

We focus here on flows generated by a deterministic forcing at large scales for which a mean flow develops in addition to turbulent fluctuations which, observations show, develop over all spatial and temporal scales.

The spectra of the dynamical run and its average in time are shown in Fig. 5a, for the DNS calculation. While the dynamical flow has a typical turbulence spectrum, the time-averaged field is sharply peaked at the size of the TG cell. As the Reynolds number varies, the characteristics of the average flow are constant (Fig. 5b). An three-dimensional representation of a snapshot in time of the kinetic energy and the time average the kinetic energy along all the simulation are shown in Fig. 6.

Now, using the time averaged velocity for static kinematic dynamo studies, we observe the existence of two dynamo branches, Fig. 7, a behavior already noted for the *ABC* flow [50]. The first dynamo mode has larger scales than

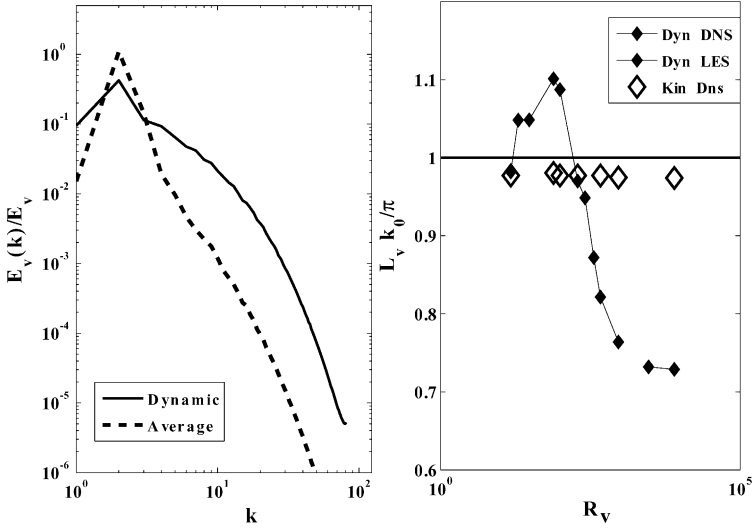


Fig. 5. (a) Kinetic energy spectra for TG1 ( $\nu = 0.007$ ,  $N = 256^3$ );  $E_{V,dyn}(k, t = T)$  (solid line),  $E_{V,kin}(k)$  (dotted line); (b): integral length scales  $L_{dyn}$  and  $L_{kin}$ , normalized by the size of the unit TG cell, versus the flow Reynolds numbers.

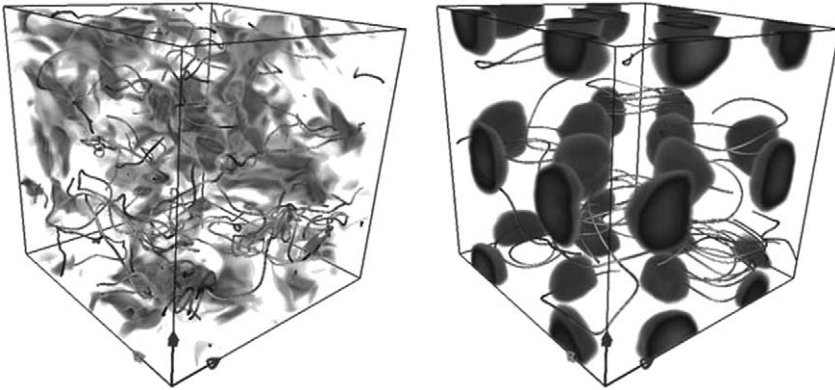


Fig. 6. (l.h.s) Snapshot of the velocity, shown in volume rendering of the kinetic energy, and some field line trajectories. the r.h.s displays the volume rendering of the kinetic energy for the time average velocity (same parameter as Fig. 4) (*imagery made with Vapor [77]*).

the fundamental box and then exist only by the collective effect of the height Taylor–Green vortex and the periodic boundaries. The second one is inside the fundamental box, and looks like the double bananas shape [72] found numeri-

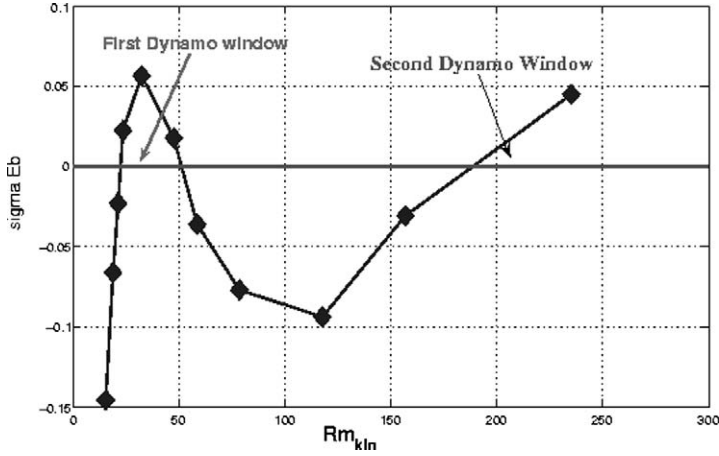


Fig. 7. Growth rates for the kinematic dynamo generated by mean flow versus the magnetic Reynolds number.

cally using the Von Kàrmàn time average velocity, recorded from water experiments [73, 74].

We compare in Fig. 8 the evolution of all  $R_M^c$  the critical magnetic Reynolds numbers. At low  $R_V$ , the dynamo threshold for the dynamical problem lies within the low  $R_M$  dynamo window for the time-averaged flow. For  $R_V$  larger than 200, the dynamical dynamo threshold lies in the immediate vicinity of the upper dynamo branch (high  $R_M^c$  mode of the time-averaged flow). It is unclear from Fig. 8 whether the effect of the fluctuations in the dynamical runs is to increase the threshold of the first kinematic window, or decrease the threshold of the second one. In the work of Laval et al. [75], some artificial noise is added to the mean flow, and by this procedure the dynamo threshold increases with the level of noise. Unfortunately the realistic velocity fluctuations are not a simple noise, so at this stage we need further works to conclude.

In the dynamical runs, the magnetic energy spectrum peaks at scales smaller, than the hydrodynamic integral scale, it is suggested that turbulent fluctuations play a role on the dynamo effect. Looking only at the magnetic spectra the Taylor–Green dynamo, it looks like a fluctuation type dynamo. But in fact the Taylor–Green dynamo is easier to obtain than fluctuation type dynamo (Fig. 1b of [76]), and the localisation of growing magnetic energy inside the neutral plan of the Taylor–Green vortex, suggest that the mean flow plays a major role in the dynamo process [72]. We can only suggest at this stage, that certainly there is a double contribution to the dynamo, the mean flow mode and some additional fluctuating dynamo process.

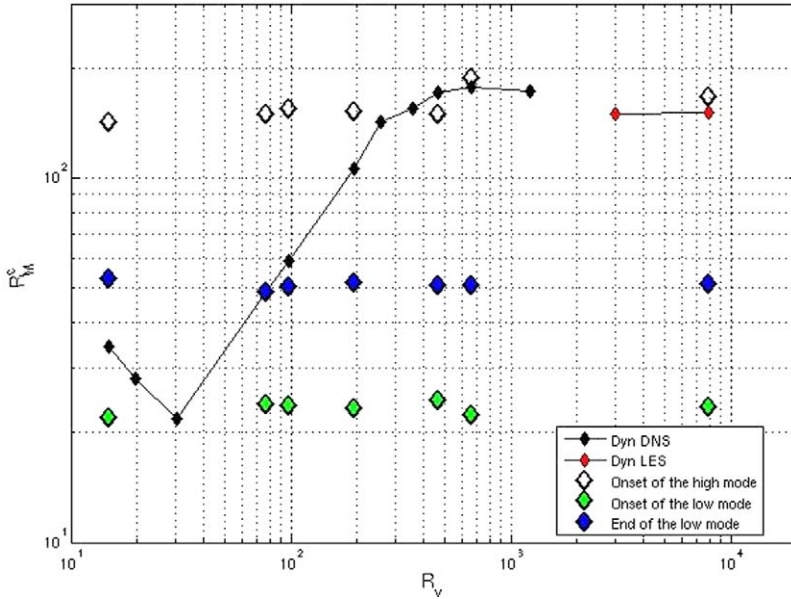


Fig. 8. Evolution of the critical magnetic Reynolds numbers for the kinematic runs from the time average velocity in diamond symbol and the dynamical runs in full line versus the Reynolds number  $R_V$ .

## 6. Non linear behavior

### 6.1. Subcritical dynamo

Previous works ([70–72, 75] or chap. 5.2) have explored the response of Taylor–Green forcing to a magnetic seed and computed the onset of the dynamo versus the Reynolds number. In the non linear regime when the magnetic field has reached sufficient amplitude, it can react back onto the velocity field, saturate the instability and reach a statistically stationary state, with approximate equipartition  $E_M \sim E_V$  (Fig. 9, with the time less then 1000).

In Fig. 9, we have quenched the system at  $t = 1000$ , the magnetic diffusivity  $\eta$  is suddenly increased by a factor of 4, lowering  $R_M$  below  $R_M^c$ . After a short transient, both  $E_V$  and  $E_M$  decrease and reach a second statistically stationary state, with a non zero magnetic energy—a new dynamo state, for which equipartition is reached again. This behavior is evidence for global subcriticality [78]. The different levels of fluctuations in the two regimes suggest the possibility of different dynamo states, depending on the magnetic field or on history of the system. As subcritical bifurcations are also associated with hysteresis cycles, we have repeated the quenching procedure starting from the same dynamo state  $A$ , and obtain a clear hysteresis cycles shown in Fig. 10.

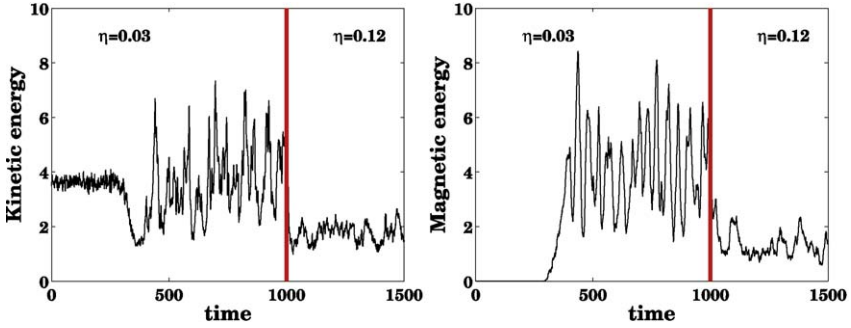


Fig. 9. After a dynamo is self-generated from infinitesimal perturbations, the induction equation is quenched at  $t = 1000$  by a four-fold increase of the magnetic diffusivity. It corresponds to a sudden change from  $A$  to  $A_9$ —cf. Fig. 10.

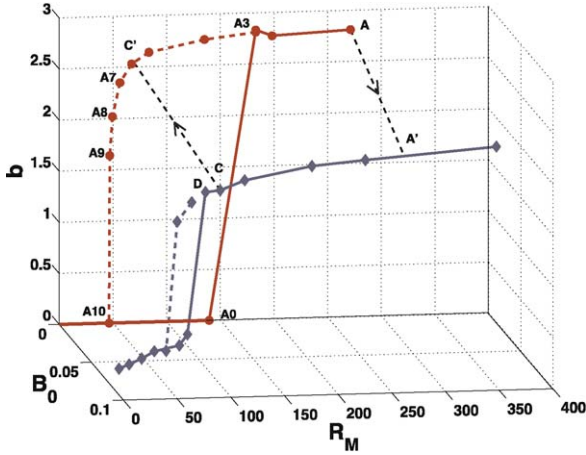


Fig. 10. Bifurcation curves and hysteresis cycles when an external magnetic field is applied (full diamond symbols) or without one (full circle symbols). In this case, the subcritical quenched states (see text) form the red line. Jumps between the two branches link  $A$  to  $A'$  and  $C$  to  $C'$ .

With an applied magnetic field the hysteresis cycle still exist but is smaller, and by changing suddenly the magnetic Reynolds number or the value of the applied magnetic field, it is possible to jump from branch to branch as Fig. 10.

A less deterministic behavior is observed when the system is operated in the vicinity of point  $D$ —shown along the blue curve in Fig. 10. We observe that the systems spontaneously switches between dynamo and non-dynamo periods, as shown in Fig. 11. This is reminiscent of the “on-off” bifurcation scenario. We present an extended example of this behavior in the next Section 6.2.

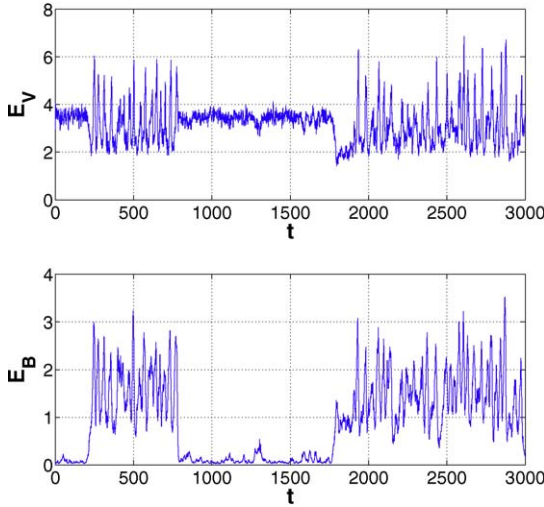


Fig. 11. Evolution in time of the kinetic ( $E_V$ ) and magnetic energy ( $E_B$ ) when the flow is occurs in the immediate vicinity of point  $D$ —see Fig. 10.

### 6.2. On-Off intermittency dynamo

On-Off intermittency has been observed in different physical experiments including electronic devices, electrohydrodynamic convection in nematics, gas discharge plasmas, and spin-wave instabilities [87]. In the MHD context, near the dynamo instability onset, the On-Off intermittency has been investigated by modeling of the Bullard dynamo [88], and experimental results have confirm a such behavior [18].

Using direct numerical simulation [84,85], they were able to observe On-Off intermittency solution of the full MHD equations for the ABC dynamo ( $F_{ABC}(k_0 = 1)$ ), (here we present an extended work of this particular case) [86].

Recent dynamo experiment results (VKS) [89] show some intermittent behavior, with features reminiscent of On-Off self-generation that motivated our study.

A simple and proven very useful way to model the behavior of the magnetic field during the on-off intermittency is using a stochastic differential equation (SDE-model) [82, 83, 90–98]:

$$\frac{\partial E_b}{\partial t} = (a + \xi)E_b - NL(E_b), \tag{6.1}$$

where  $E_b$  is the magnetic energy,  $a$  is the long time averaged growth rate,  $\xi$  models the noise term typically assumed to be white (see however [97, 98]) and of amplitude  $D$  such that  $\langle \xi(t)\xi(t') \rangle = 2D\delta(t - t')$ .  $NL$  is a non-linear

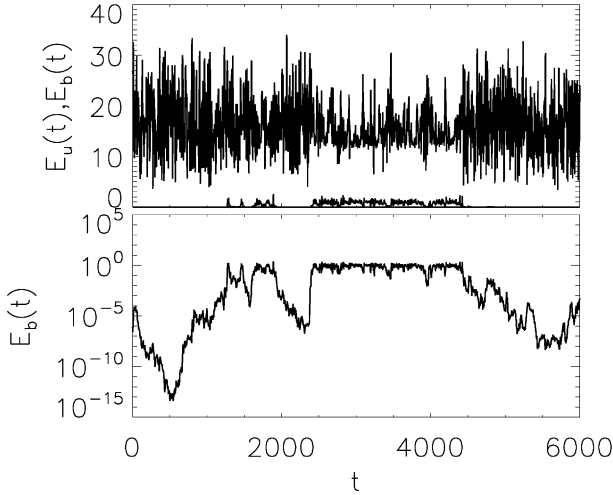


Fig. 12. A typical example of a burst. The top panel shows the evolution of the kinetic energy (top line) and magnetic energy (bottom line). The bottom panel shows the evolution of the magnetic energy in a log-linear plot. During the on phase of the dynamo the amplitude of the noise of the kinetic energy fluctuations is significantly reduced.

term that guaranties the saturation of the magnetic energy to finite values typically taken to be  $NL(X) = X^3$  for investigations of supercritical bifurcations or  $NL(X) = X^5 - X^3$  for investigations of subcritical bifurcations. In all these cases (independent of the non-linear saturation mechanism) the above SDE leads to stationery distribution function that for  $0 < a < D$  has a singular behavior at  $E_b = 0$ :  $P(E_b) \sim E_b^{a/D-1}$  indicating that the systems spends a lot of time in the neighborhood of  $E_b = 0$  [93–96].

In the dynamical system eq. (6.1) studied, the noise amplitude or the noise proprieties do not depend on the amplitude of the magnetic energy.

However, in the MHD system, when the non-linear regime is reached, the Lorentz force has a clear effect on the flow by decreasing the small scale fluctuations, and decreases of the local Lyapunov exponent [79, 80]. In some cases, the flow is altered so strongly that the MHD dynamo system jumps into an other attractor, that cannot not no longer sustain the dynamo instability [81]. Although the exact mechanism of the saturation of the MHD dynamo is still an open question that might not have a universal answer, it is clear that both the large scales and the turbulent fluctuations are altered in the non-linear regime and need to be accounted in a model.

Figure 12 demonstrates this point, by showing the evolution of the kinetic and magnetic energy as the dynamo goes through On- and Off- phases. During

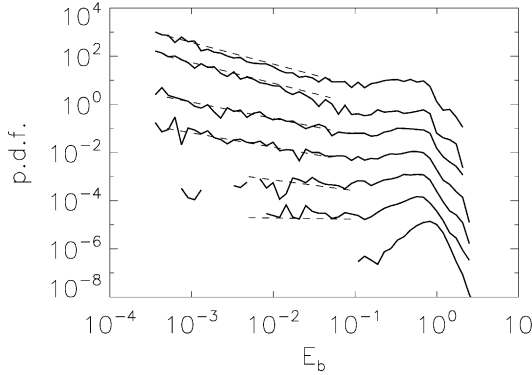


Fig. 13. The probability distribution functions of  $E_b$ , at seven different values of the magnetic Reynolds number. The last case shows no on-off intermittency. The dashed lines show the prediction of the SDE model.

the On phases, the mean value and the amplitude of the observed fluctuations of the kinetic energy are significantly reduced. As a result the On-phases last a lot longer than the SDE-model would predict. The effect of the long duration of the “On” times can also be seen in the pdfs of the magnetic energy. The probability distribution function (pdf) for the examined magnetic Reynolds number are shown in Fig. 13. For different values of the magnetic Reynolds number the pdf of the magnetic field is concentrated at large values  $E_b \simeq 1$  producing a peak in the pdf curves. When the magnetic Reynolds number increases the On-Off power law disappears.

This peak can be attributed to the quenching of the hydrodynamic “noise” in the nonlinear stage. In principle the SDE model eq. (6.1) can be modified to include this effect: using an energy  $E_b$  depending of the amplitude of the noise. There many possible ways to model the quenching of the noise, however the nonlinear behavior might not be a universal behavior and we do not attempt to suggest a specific model.

## 7. Perspective

The periodic box remains an attractive tool to study MHD turbulence and the impact of velocity fluctuation on the dynamo onset. The absence of boundary condition could be modelled by new techniques introduced in pseudo-spectral codes such as the penalisation method [99] or pseudo-penalisation method [100]. The classical wish in the numerical simulation is generally to increase the resolution to reach high Reynolds numbers. But there is a more challenging limit which is

more relevant to dynamo experiment: to massively increase the run time of the simulations. Indeed, the dynamo experiments easily reach a thousand magnetic diffusion time ( $\Delta T \sim 1000 \tau_\eta$ ). If we want to be able to compare data statistically between the experiments and the simulations, the simulation time needs to be extended ( $\Delta T \sim 1000 R_m \tau_{NL}$ ) between ten thousand to hundred thousand of hydrodynamic eddy turn over time.

## 8. Acknowledgements

YP acknowledges the co-authors of our common articles [49, 70, 72, 78, 86] which represent the basis of this lecture (A. Pouquet, J-F Pinton, H. Politano, A. Alexakis, P. Mininni, J-P Laval, B. Dubrulle and F. Daviaud). All work presented here is supported by the French GDR Dynamo and the computer time was provided by IDRIS and the Mesocentre SIGAMM at Observatoire de la Côte d'Azur. YP thanks A. Miniussi for computing design assistance and M.S Rosin for reading and improving this manuscript. YP is grateful to the summer school organisers to give him the opportunity to have fruitful discussions with the lecturers and promising students, and spend great time with the family (Annick, Florian, Julien and Scooby (dog)).

## References

- [1] H.K. Moffatt, *Magnetic Field Generation in Electrically Conducting Fluids*, Cambridge University Press, Cambridge, 1978; F. Krause and K.-H. Radler, *Mean-Field Magnetohydrodynamics and Dynamo Theory*, Pergamon, Oxford, 1980; E.N. Parker, *Cosmical Magnetic Fields*, Clarendon, Oxford, 1979.
- [2] A. Gailitis, O. Lielausis, S. Dement'ev, E. Platacis, A. Cifersons, G. Gerbeth, T. Gundrum, F. Stefani, M. Christen, H. Hänel and G. Will, Detection of a flow induced magnetic field eigenmode in the Riga dynamo facility, *Phys. Rev. Lett.* **84**, 4365 (2000).
- [3] A. Gailitis, O. Lielausis, S. Dement'ev, A. Cifersons, G. Gerbeth, T. Gundrum, F. Stefani, M. Christen, H. Hänel and G. Will, Magnetic field saturation in the Riga dynamo experiment, *Phys. Rev. Lett.* **86**, 3024 (2001).
- [4] A. Gailitis, O. Lielausis, E. Platacis, G. Gerbeth and F. Stefani, Riga dynamo experiment and its theoretical background, *Physics of Plasmas* **11**(5), 2838–2843 (2004).
- [5] U. Müller and R. Stieglitz, *Naturwissenschaften* **87**, 381 (2000).
- [6] R. Stieglitz and U. Müller, Experimental demonstration of a homogeneous two-scale dynamo, *Phys. Fluids* **13**, 561 (2001).
- [7] R. Monchaux, M. Berhanu, M. Bourgoin, M. Moulin, Ph. Odier, J.-F. Pinton, R. Volk, S. Fauve, N. Mordant, F. Pétrélis, A. Chiffaudel, F. Daviaud, B. Dubrulle, C. Gasquet, L. Marié and F. Ravelet, Generation of a magnetic field by dynamo action in a turbulent flow of liquid sodium, *Phys. Rev. Lett.* **98**, 044502 (2007).

- [8] M. Berhanu, R. Monchaux, S. Fauve, N. Mordant, F. Pétrélis, A. Chiffaudel, F. Daviaud, F. Ravelet, M. Bourgoïn, Ph. Odier, J.-F. Pinton, R. Volk, B. Dubrulle and L. Marie, Magnetic field reversals in an experimental turbulent dynamo, *Europhys. Lett.* **77**, 59001 (2007).
- [9] P. Odier, J.-F. Pinton and S. Fauve, Advection of a magnetic field by a turbulent swirling flow, *Phys. Rev. E* **58**, 7397–7401 (1998).
- [10] N.L. Peffley, A.B. Cawthorne and D.P. Lathrop, Toward a self-generating magnetic dynamo, *Phys. Rev. E* **61**, 5287 (2000).
- [11] N.L. Peffley, A.G. Goumilevski, A.B.C. and D.P. Lathrop, Characterization of experimental dynamos, *Geoph. J. Int.* **142**, 52–58 (2000).
- [12] P. Frick, V. Noskov, S. Denisov, S. Khripchenko, D. Sokoloff, R. Stepanov and A. Sukhanovsky, Non-stationary screw flow in a toroidal channel: way to a laboratory dynamo experiment, *Magneto-hydrodynamics* **38**(1/2), 143–162 (2002).
- [13] M. Bourgoïn, L. Marié, F. Pétrélis, C. Gasquet, A. Guiguon, J.-B. Luciani, M. Moulin, F. Namer, J. Burguete, F. Daviaud, A. Chiffaudel, S. Fauve, Ph. Odier and J.-F. Pinton, MHD measurements in the von Kármán sodium experiment, *Phys. Fluids* **14**, 3046 (2002).
- [14] M.D. Nornberg, E.J. Spence, R.D. Kendrick, C.M. Jacobson and C.B. Forest, Intermittent magnetic field excitation by a turbulent flow of liquid sodium, *Phys. Rev. Lett.* **97**, 044503 (2006).
- [15] M.D. Nornberg, E.J. Spence, R.D. Kendrick and C.B. Forest, Measurements of the magnetic field induced by a turbulent flow of liquid metal, *Phys. Plasmas* **13**, 055901 (2006).
- [16] R. Stepanov, R. Volk, S. Denisov, P. Frick, V. Noskov and J.-F. Pinton, Induction, helicity and alpha effect in a toroidal screw flow of liquid gallium, *Phys. Rev. E* **73**, 046310 (2006).
- [17] R. Volk, P. Odier and J.-F. Pinton, Fluctuation of magnetic induction in von Kármán swirling flows, *Phys. Fluids* **18**, 085105 (2006).
- [18] M. Bourgoïn, R. Volk, N. Plihon, P. Augier, P. Odier and J.-F. Pinton, An experimental Bullard-von Kármán dynamo, *New Journal of Physics* **8**, 329 (2006).
- [19] A. Gailitis et al., Project of a liquid Sodium MHD dynamo experiment, *Magneto-hydrodynamics* **1**, 63 (1996).
- [20] A. Tilgner, A kinematic dynamo with a small scale velocity field, *Phys. Rev. A* **226**, 75 (1997).
- [21] L. Marié, J. Burguete, F. Daviaud and J. Léorat, *Eur. J. Phys. B* **33**, 469 (2003); F. Ravelet et al., *Phys. Fluids* **17**, 117104 (2005).
- [22] R.A. Bayliss, C.B. Forest and P.W. Terry, Numerical simulations of current generation and dynamo excitation in a mechanically forced turbulent flow, *Phys. Rev. Lett.* **75**, 026303–13 (2007).
- [23] S. Kenjereš and K. Hanjalić, Numerical simulation of a turbulent magnetic dynamo, *Phys. Rev. Lett.* **98**, 104501 (2007).
- [24] S. Kenjereš and K. Hanjalić, Numerical insights into magnetic dynamo action in a turbulent regime, *New J. Phys.* **9**, 306 (2007).
- [25] J.L. Guermond, J. Léorat and C. Nore, A new Finite Element Method for magneto-dynamical problems: two-dimensional results, *E. J. Mech. Fluids* **22**, 555 (2003).
- [26] J.L. Guermond, R. Laguerre, J. Léorat and C. Nore, An interior penalty Galerkin method for the MHD equations in heterogeneous domains, *J. Comp. Phys.* **221**, 349–369 (2007).
- [27] A.B. Iskakov, S. Descombes and E. Dormy, An integro-differential formulation for magnetic induction in bounded domains: boundary element-finite volume method, *J. Comp. Phys.* **197**, 540–554 (2004).
- [28] A.B. Iskakov and E. Dormy, On magnetic boundary conditions for non-spectral dynamo simulations, *Geophys. Astrophys. Fluid Dyn.* **99**, 481–492 (2006).

- [29] U. Frisch, *Turbulence: The Legacy of A.N. Kolmogorov*, Cambridge University Press, 1996.
- [30] M. Lesieur, *Turbulence in Fluids*, Kluwer, 1997.
- [31] A. Vincent and M. Meneguzzi, The spatial structure and the statistical properties of homogeneous turbulence, *J. Fluid Mech.* bf 225, 1–25 (1991).
- [32] S.A. Orszag, Numerical methods for the simulation of turbulence, *Phys. of Fluid* **21**(Suppl. II), 250–257 (1969).
- [33] C. Canuto, M.Y. Hussaini, A. Quarteroni and T.A. Zang, *Spectral methods in Fluid Dynamics*, Springer-Verlag, 1988.
- [34] R. Peyret, *Spectral Method for Incompressible Viscous Flow*, Applied Mathematical Sciences, vol. 148, Springer, 2002.
- [35] S.A. Orszag, Comparison of pseudospectral and spectral approximations, *Stud. Appl. Math.* **51** (1972).
- [36] S.A. Orszag and J.S. Patterson Jr., Numerical simulation of three-dimensional homogeneous isotropic turbulence, *Phys. Rev. Lett.* **28**, 76–79 (1972).
- [37] M.E. Brachet, D.I. Meiron, S.A. Orszag, B.G. Nickel, R.H. Morf and U. Frisch, Small-scale structure of the Taylor–Green vortex, *J. Mech. Fluids* **130**, 411–452 (1983).
- [38] V.I. Arnold, *Comptes Rendus Acad. Sci. Paris* **261**, 17 (1965).
- [39] T. Dombre, U. Frisch, J.M. Greene, M. Henon, A. Mehr and A. Soward, Chaotic streamlines in the ABC flows, *J. Fluid Mech.* **167**, 353 (1986).
- [40] C. Basdevant, Le modèle de simulation numérique de turbulence bidimensionnelle du L.M.D, Note interne LMD no 114, laboratoire de Météorologie Dynamique du CNRS, Paris, 1982.
- [41] Y. Kaneda, T. Ishihara, M. Yokokawa, K. Itakura and A. Uno, Energy dissipation rate and energy spectrum in high resolution direct numerical simulations of turbulence in a periodic box, *Phys. Fluids* **15**, L21–L24 (2003).
- [42] M. Lesieur and O. Métais, *Ann. Rev. Fluid Mech.* **28**, 45 (1996).
- [43] C. Meneveau and J. Katz, *Annu. Rev. Fluid Mech.* **32**, 1 (2000).
- [44] U. Piomelli, *Prog. Aerosp. Eng.* **35**, 335 (1999).
- [45] P. Sagaut, *Large Eddy Simulation for Incompressible Flows*, 2nd ed., Springer-Verlag, Berlin, 2003.
- [46] J.P. Chollet and M. Lesieur, Parameterisation for small scales of three dimensional isotropic turbulence using spectral closure, *J. Atmos. Sci.* **38**, 2747 (1981).
- [47] O. Métais, Large-Eddy Simulations of Turbulence, in: *New trends in turbulence. Turbulence: nouveaux aspects Les Houches Session LXXIV 31 July–1 September 2000, Series: Les Houches—Ecole d’Ete de Physique Theorique*, Vol. 74, Lesieur, M., Yaglom, A., David, F., eds., Springer Jointly published with EDP Sciences, Les Ulis.
- [48] J. Baerenzung, H. Politano, Y. Ponty and A. Pouquet, Spectral modeling of turbulent flows and the role of helicity, *Phys. Rev. E* under press (2008) (available arXiv:0707.0642).
- [49] Y. Ponty, J. F Pinton and H. Politano, Simulation of induction at low magnetic Prandtl number, *Phys. Re. Lett.* **92** 14, 144503 (2004).
- [50] D.J. Galloway and M.R.E. Proctor, Numerical calculations of fast dynamo for smooth velocity field with realistic diffusion, *Nature* **356**, 691–693 (1992).
- [51] Y. Ponty, A. Pouquet and P.L. Sulem, Dynamos in weakly chaotic 2-dimensional flows, *Geophys. Astrophys. Fluid Dyn.* **79**, 239–257 (1995).
- [52] V.I. Arnold and E.I. Korkina, The grow of magnetic field in a incompressible flow, *Vestn. Mosk. Univ. Mat. Mekh.* **3**, 43–46 (1983).
- [53] D.J. Galloway and U. Frisch, Dynamo action in a family of flows with chaotic stream lines, *Geophys. Astrophys. Fluid Dyn.* **36**, 53–83 (1986).

- [54] B. Galanti, P.L. Sulem and A. Pouquet, Linear and non-linear dynamos associated with the ABC flow, *Geophys. Astrophys. Fluid Dyn.* **66**, 183–208 (1992).
- [55] V. Archontis, S.B.F. Dorch and A. Nordlund, Numerical simulations of kinematic dynamo action, *Astron. Astrophys.* **397**, 393–399 (2003).
- [56] R. Teyssier, S. Fromang and E. Dormy, Kinematic dynamos using constrained transport with high order Godunov schemes and adaptive mesh refinement, *J. Comp. Dyn.* **218**, 44–67 (2006).
- [57] S. Childress and A.D. Gilbert, *Stretch, Twist Fold: The Fast Dynamo*, Springer-Verlag, New York, 1995.
- [58] H.K. Moffat and M.R. Proctor, Topological constraints associated with fast dynamo action, *J. Fluid Mech.* **154**, 493 (1985).
- [59] B.J. Bayly and S. Childress, *Geophys. Astrophys. Fluid Dyn.* **44**, 211 (1988).
- [60] J.M. Finn and E. Ott, Chaotic flows and fast magnetic dynamos, *Phys. Fluids* **31**, 2992 (1988).
- [61] J.M. Finn and E. Ott, Chaotic flows and magnetic dynamos, *Phys. Rev. Lett.* **60**, 760 (1988).
- [62] O.M. Podvigina and A. Pouquet, On the nonlinear stability of the  $1 = 1 = 1$  ABC flow, *Physica D* **75**, 471–508 (1994).
- [63] O.M. Podvigina, Spatially-periodic steady solutions to the three-dimensional Navier–Stokes equation with the ABC-force, *Physica D* **128**, 250–272 (1999).
- [64] P. Ashwin and O. Podvigina, Hopf bifurcation with cubic symmetry and instability of ABC flow, *Proc. R. Soc. London* **459**, 1801–1827 (2003).
- [65] O. Podvigina, P. Ashwin and D.J. Hawker, Modelling instability of ABC flow using a mode interaction between steady and Hopf bifurcations with rotational symmetries of the cube, *Physica D* **215**, 62–79 (2006).
- [66] P.D. Mininni, Turbulent magnetic dynamo excitation at low magnetic Prandtl number, *Physics of Plasmas* **13**(5), 056502 (2006).
- [67] S. Douady, Y. Couder and M.-E. Brachet, Direct observation of the intermittency of intense vorticity filaments in turbulence, *Phys. Rev. Lett.* **67**, 983 (1991).
- [68] C. Nore, M. Brachet, H. Politano and A. Pouquet, Dynamo action in the Taylor–Green vortex near threshold, *Phys. Plasmas* **4**, 1 (1997).
- [69] C. Nore, M.-E. Brachet, H. Politano and A. Pouquet, Dynamo action in a forced Taylor–Green vortex, in: *Dynamo and Dynamics, a Mathematical Challenge*, NATO Science Series II, vol. 26, P. Chossat, D. Armbruster and I. Oprea, eds., Kluwer Academic, Dordrecht, 2001. Proceedings of the NATO Advanced Research Workshop, Cargèse, France, 21–26 August 2000, pp. 51–58.
- [70] Y. Ponty, P.D. Mininni, A. Pouquet, H. Politano, D.C. Montgomery and J.-F. Pinton, Numerical study of dynamo action at low magnetic Prandtl numbers, *Phys. Rev. Lett.* **94**, 164512 (2005).
- [71] P.D. Mininni, Y. Ponty, D.C. Montgomery, J.-F. Pinton, H. Politano and A. Pouquet, Dynamo regimes with a non-helical forcing, *The Astrophysical Journal* **626**, 853–863 (2005).
- [72] Y. Ponty, P.D. Mininni, J.-F. Pinton, H. Politano and A. Pouquet, Dynamo action at low magnetic Prandtl numbers: mean flow *versus* fully turbulent motions, *New J. Phys.* **9**, 296 (2007).
- [73] F. Ravelet, A. Chiffaudel, F. Daviaud and J. Léorat, Toward an experimental von Kármán dynamo: Numerical studies for an optimized design, *Phys. Fluids* **17**, 117104 (2005).
- [74] F. Ravelet, A. Chiffaudel, F. Daviaud and L. Marié, Multistability and memory effect in a highly turbulent flow: experimental evidence for a global bifurcation, *Phys. Rev. Letters* **93**, 164501 (2004).
- [75] J.-P. Laval, J.-P. Blaineau, N. Leprovost, B. Dubrulle and F. Daviaud, Influence of turbulence on the dynamo threshold, *Phys. Rev. Lett.* **96**, 204503 (2006).

- [76] A.A. Schekochihin, A.B. Iskakov, S.C. Cowley, J.C. McWilliams, M.R.E. Proctor and T.A. Yousef, Fluctuation dynamo and turbulent induction at low magnetic Prandtl numbers, *New J. Phys.* **9**, 300 (2007).
- [77] Imagery using VAPOR code ([www.vapor.ucar.edu](http://www.vapor.ucar.edu)) a product of the National Center for Atmospheric Research.
- [78] Y. Ponty, J.-P. Laval, B. Dubrulle, F. Daviaud and J.-F. Pinton, Subcritical dynamo bifurcation in the Taylor–Green Flow, *Phys. Rev. Lett.* **99**, 224501 (2007).
- [79] F. Cattaneo, D.W. Hughes and E.J. Kim, Suppression of chaos in a simplified nonlinear dynamo model, *Phys. Rev. Lett.* **76**, 2057–2060 (1996).
- [80] E. Zienicke, H. Politano and A. Pouquet, Variable intensity of Lagrangian chaos in the nonlinear dynamo problem, *Phys. Rev. Lett.* **81**, 4640–4640 (1998).
- [81] N.H. Brummell, F. Cattaneo and S.M. Tobias, Linear and nonlinear dynamo properties of time-dependent ABC flows, *Fluid Dynamics Research* **28**, 237–265 (2001).
- [82] Y. Pomeau and P. Manneville, Intermittent transition to turbulence in dissipative dynamical systems, *Commun. Math. Phys.* **74**, 1889 (1980).
- [83] N. Platt, E.A. Spiegel and C. Tresser, On-off intermittency: A mechanism for bursting, *Phys. Rev. Lett.* **70**(3), 279–282 (1993).
- [84] D. Sweet, E. Ott, J.M. Finn, T.M. Antonsen, Jr. and D.P. Lathrop, Blowout bifurcations and the onset of magnetic activity in turbulent dynamos, *Phys. Rev. E* **63**, 066211 (2001).
- [85] D. Sweet, E. Ott, T.M. Antonsen, Jr. and D.P. Lathrop, J.M. Finn, Blowout bifurcations and the onset of magnetic dynamo action, *Physics of Plasmas* **8**, 1944–1952 (2001).
- [86] A. Alexakis and Y. Ponty, The Lorentz force effect on the On-Off dynamo intermittency, under press, *Phys. Rev. E* (available: <http://fr.arxiv.org/abs/0710.0063> arXiv:0710.003).
- [87] A.S. Pikovsky, *Z. Phys. B* **55**, 149 (1984); P.W. Hammer, N. Platt, S.M. Hammel, J.F. Heagy and B.D. Lee, *Phys. Rev. Lett.* **73**(8), 1095–1098 (1994). T. John, R. Stannarius and U. Behn, *Phys. Rev. Lett.* **83**(4), 749–752 (1999); D.L. Feng, C.X. Yu, J.L. Xie and W.X. Ding, *Phys. Rev. E* **58**(3), 3678–3685 (1998); F. Rodelsperger, A. Cenys and H. Benner, *Phys. Rev. Lett.* **75**(13), 2594–2597 (1995).
- [88] N. Lévêque, B. Dubrulle and F. Plunian, Intermittency in the homopolar disc-dynamo, *Magneto-hydrodynamics* **42**, 131–142 (2006).
- [89] VKS Private communication, Les Houches, August 2007.
- [90] H. Fujisaka and T. Yamada, *Prog. Theor. Phys.* **74**(4), 918–921 (1984); H. Fujisaka, H. Ishii, M. Inoue and T. Yamada, *Prog. Theor. Phys.* **76**(6), 1198–1209 (1986).
- [91] E. Ott and J.C. Sommerer, *Phys. Lett. A* **188**, 39 (1994).
- [92] L. Yu, E. Ott and Q. Chen, *Phys. Rev. Lett.* **65**, 2935 (1990).
- [93] N. Platt, S.M. Hammel and J.F. Heagy, *Phys. Rev. Lett.* **72**, 3498 (1994).
- [94] J.F. Heagy, N. Platt and S.M. Hammel, *Phys. Rev. E* **49**, 1140 (1994).
- [95] S.C. Venkataramani, T.M. Antonsen, Jr., E. Ott and J.C. Sommerer, *Phys. Lett. A* **207**, 173 (1995).
- [96] S.C. Venkataramani, T.M. Antonsen, Jr., E. Ott and J.C. Sommerer, *Physica D* **96**, 66 (1996).
- [97] S. Aumaître, F. Pétrélis and K. Mallick, Low-frequency noise controls on-off intermittency of bifurcating systems, *Phys. Rev. Lett.* **95**, 064101 (2005).
- [98] S. Aumaître, K. Mallick and F. Pétrélis, Effects of the low frequencies of Noise on On-Off intermittency, *Journal of Statistical Physics*, **123**, 909–927 (2006).
- [99] K. Schneider and M. Farge, Decaying two-dimensional turbulence in a circular container, *Phys. Rev. Lett.* **95**, 244502 (2005).
- [100] R. Pasquetti, R. Bwemba and L. Cousin, A pseudo-penalization method for high Reynolds number unsteady flows, *Applied Numerical Mathematics* **33**, 207–216 (2007).